Draft version July 24, 2013
Preprint typeset using LaTeX style emulateapj v. 04/03/99

arXiv:astro-ph/0401432v1 21 Jan 2004

X-RAY AND RADIO EMISSION FROM UV-SELECTED STAR FORMING GALAXIES AT REDSHIFTS $1.5 \lesssim Z \lesssim 3.0$ IN THE GOODS-NORTH FIELD[1]

Naveen A. Reddy & Charles C. Steidel
California Institute of Technology, MS 105–24, Pasadena, CA 91125; nar@astro.caltech.edu, ccs@astro.caltech.edu
DRAFT: July 24, 2013

ABSTRACT

We have examined the stacked radio and X-ray emission from UV-selected galaxies spectroscopically confirmed to lie between redshifts $1.5 \lesssim z \lesssim 3.0$ in the GOODS-North field to determine their average extinction and star formation rates (SFRs). The X-ray and radio data are obtained from the Chandra 2 Msec survey and the Very Large Array, respectively. There is a good agreement between the X-ray, radio, and de-reddened UV estimates of the average SFR for our sample of $z \sim 2$ galaxies of ~ 50 M$_\odot$ yr^{-1}, indicating that the locally-calibrated SFR relations appear to be statistically valid from redshifts $1.5 \lesssim z \lesssim 3.0$. We find that UV-estimated SFRs (uncorrected for extinction) underestimate the bolometric SFRs as determined from the $2-10$ keV X-ray luminosity by a factor of $\sim 4.5-5.0$ for galaxies over a large range in redshift from $1.0 \lesssim z \lesssim 3.5$.

Subject headings: galaxies: evolution—-galaxies: high-redshift—galaxies: starburst—dust, extinction—radio continuum: galaxies—X-rays: galaxies

1. INTRODUCTION

Estimating global star formation rates (SFRs) of galaxies typically requires using relations that can be quite uncertain as they incorporate a large number of assumptions in converting between specific and bolometric luminosities (e.g., assumed IMF, extinction, etc.; e.g., Adelberger & Steidel 2000). The varied efforts in the Great Observatories Origins Deep Survey (GOODS; Giavalisco et al. 2003) allow us to examine the same galaxies over a broad range of wavelengths to mitigate some of these uncertainties. X-ray, radio, and UV emission are all thought to directly result from massive stars and are consequently used as tracers of current star formation (e.g., Ranalli, Comastri, & Setti 2003; Condon 1992; Gallego et al. 1995). Here we use the X-ray, radio, and UV emission, each differently affected by extinction (or not at all), to determine SFRs of galaxies at $z \sim 2$.

Observations of the QSO and stellar mass density, and morphological diversification all point to the epoch around $z \sim 2$ as an important period in cosmic history (e.g., Di Matteo et al. 2003; Chapman et al. 2003). Until recently, this epoch has been largely unexplored as lines used for redshift identification are shifted to the near-UV where detector sensitivity has been poor or to the near-IR, where spectroscopy is more difficult due to higher backgrounds. With the recent commissioning of the blue side of the Low Resolution Imaging Spectrograph (LRIS; Oke et al. 1995) on the Keck I telescope, we have for the first time been able to obtain spectra for large numbers of galaxies at these redshifts. Adding to the multi-wavelength efforts in the GOODS-North field, we have undertaken a program to identify photometric candidates in this field between $1.5 \lesssim z \lesssim 3.0$ and perform followup spectroscopy with LRIS-B (Steidel et al. 2004). This UV-selected sample of galaxies forms the basis for our subsequent multi-wavelength analysis.

Current sensitivity limits at X-ray and radio wavelengths preclude the direct detection of normal star forming galaxies at $z \gtrsim 1.5$. Nonetheless, we can use a "stacking" procedure to effectively add the emission from a class of objects in order to determine their average emission properties (e.g., Nandra et al. 2002; Brandt et al. 2001; Seibert, Heckman, & Meurer 2002). In this paper, we present a stacking analysis of the radio and X-ray emission from UV-selected star forming galaxies at redshifts $1.5 \lesssim z \lesssim 3.0$ to cross-check three different techniques of estimating SFRs at high redshifts. $H_o = 70$ km s^{-1} Mpc^{-1}, $\Omega_{\rm M} = 0.3$, and $\Omega_\Lambda = 0.7$ are assumed throughout.

2. DATA

The techniques for selecting galaxies at $z \sim 2$ are designed to cover the same range of UV properties and extinction to those used to select Lyman-break galaxies (LBGs) at higher redshifts ($z \gtrsim 3.0$; Adelberger et al. 2004). Here, we simply mention that we have two spectroscopic samples at $1.5 \lesssim z \lesssim 2.5$: a "BX" sample of galaxies selected on the expected $U_{\rm n}G\mathcal{R}$ colors of LBGs redshifted to $2.0 \lesssim z \lesssim 2.5$; and a "BM" sample targeting $z \sim 1.5-2.0$. (see Adelberger et al. 2004 and Steidel et. al. 2004 for a complete description). We presently have 138 redshifts ($\langle z \rangle \sim 2.2 \pm 0.3$) and 48 redshifts ($\langle z \rangle \sim 1.7 \pm 0.3$) in the GOODS-North BX and BM samples, respectively.

The X-ray data are from the Chandra 2 Msec survey of the GOODS-North region (Alexander et al. 2003). We made use of their raw images and exposure maps in the Chandra soft X-ray band ($0.5-2.0$ keV). Dividing the raw image by the appropriate exposure map yields an image with the count rates corrected for vignetting, exposure time, and variations in instrumental sensitivity. The on-axis soft band sensitivity is $\sim 2.5 \times 10^{-17}$ ergs cm^{-2} s^{-1} ($3\,\sigma$).

The radio data are from the Richards (2000) Very Large Array (VLA) survey of the Hubble Deep Field North (HDF-N), reaching a $3\,\sigma$ sensitivity of $\sim 23\,\mu$Jy beam^{-1} at 1.4 GHz. The final naturally-weighted image has a pixel size of $0\farcs4$ and resolution of $2\farcs0$, with astrometric accuracy of $< 0\farcs03$.

3. STACKING PROCEDURE

We divided the spectroscopic data into subsets based on selection (BX and BM) and redshift, removed sources with matching X-ray or radio counterparts within 2.″5 (or sources whose apertures are large enough to contain emission from a nearby extended X-ray or radio source), and stacked galaxies in these subsets. Four of the removed x-ray/radio sources are detected at 850 μm with SCUBA.

The X-ray data were stacked using the following procedure. We added the flux within apertures randomly dithered by 0.″5 at the positions of the galaxies (targets) in the X-ray images to produce a signal. Similarly-sized apertures were randomly placed within 5″ of the galaxy positions to sample the local background near each galaxy while avoiding known X-ray sources. This was repeated 1000 times to estimate the mean signal and background. The Chandra PSF widens for large angles from the average pointing (off-axis angle), and we fixed the aperture sizes to the 50% encircled energy (EE) radii (Feigelson et al. 2002) for off-axis angles $> 6'$. Background included at large off-axis angles becomes significant due to increasing aperture size and this can degrade the total stacked signal. Consequently, we only stacked galaxies within the off-axis angle that results in the highest S/N (this varies for each subsample, from 6 to 8′). Including all sources in the stack reduces the S/N but does not affect the absolute flux value. For sources $< 6'$ from the pointing center, the 50% EE radius falls below 2.″5, and we adopted a fixed 2.″5 radius aperture to avoid the possibility of placing an aperture off a target as a result of dithering or astrometric errors—which are $\sim 0.''3$—for sources very close to the average pointing. Stacking was performed on both the raw and normalized images to calculate the S/N and total count rate, respectively. Aperture corrections were applied to the raw counts and count rate. The conversion between count rate and flux was determined by averaging the count rate to flux conversions for the 74 optically bright X-ray sources in the catalogs of Alexander et al. (2003; Table 7) which are assumed to have a photon index of $\Gamma = 2.0$, typical of the X-ray emission from star forming regions (e.g., Kim, Fabbiano, & Trinchieri 1992; Nandra et al. 2002), and incorporate corrections for the QE degredation of the ACIS-I chips. In converting flux to rest-frame luminosity, we assume $\Gamma = 2.0$ and a Galactic absorption column density of $N_{\rm H} = 1.6 \times 10^{20}$ cm^{-2} (Stark et al. 1992). Uncertainties in flux and luminosity are dominated by Poisson noise and not the dispersion in measured values for each stacking repetition, so we assume the former.

To stack the radio data, we extracted sub-images at the locations of the targets from the mosaicked radio data of Richards (2000). These were corrected for the primary beam attenuation of the VLA with a maximum gain correction of 15%, coadded using a $1/\sigma^2$ weighted average to produce a stacked signal with maximal $S/N \sim 4.5$, and smoothed by 1.″5. The integrated flux density, $S_{1.4\,\rm GHz}$, and error were computed from the standard AIPS[2] task JMFIT using an elliptical gaussian to model the stacked emission. We assume a synchrotron spectral index of $\gamma = -0.8$, typical of the non-thermal radio emission from star forming galaxies (Condon 1992). Results of the X-ray and radio stacks for various subsamples are presented in Table 1. Four subsamples contain too few sources to yield a robust estimate of the stacked radio flux.

[2]AIPS is the Astronomical Image Processing System software package written and supported by the National Radio Astronomy Observatory.

4. RESULTS AND DISCUSSION

4.1. *SFR Estimates*

The relations established at $z = 0$ to convert luminosities to SFRs for our $z \sim 2$ sample are adopted from the following sources: Kennicutt (1998a,b) for conversion of the $1500 - 2800$ Å luminosity; Ranalli et al. (2003) for the $2 - 10$ keV luminosity; and Yun, Reddy, & Condon (2001) for the 1.4 GHz luminosity. These relations must be used with caution when applied to individual galaxies given uncertainties in the SFR relations (e.g., burst age, IMF) as well as the factor of ~ 2 dispersion in the correlations between different specific luminosities. However, they should yield reasonable results when applied to an ensemble of galaxies, as we have done here.

Table 2 shows the SFR estimates based on the $2-10$ keV ("$\rm SFR_X$"), 1.4 GHz ("$\rm SFR_{1.4\ GHz}$"), and UV ("$\rm SFR_{UV}$") luminosities, with typical error of $\sim 20\%$. We approximate the UV luminosity by using the 1600 Å rest-frame flux for all samples except the highest redshift bin sample ($2.5 < z \lesssim 3.0$) where we use the 1800 Å rest-frame flux. UV-estimated SFRs were corrected for extinction using the observed $G - \mathcal{R}$ colors, a spectral template assuming constant star formation for $> 10^8$ yr (after which the UV colors are essentially constant), and applying the reddening law of Calzetti et al. (2000) and Meurer, Heckman, & Calzetti (1999). We created 4 additional subsamples of galaxies according to de-reddened UV-estimated SFR, also shown in Table 2.

4.2. *Stacked Galaxy Distribution and AGN*

Stacking only indicates the average emission properties of galaxies, not their actual distribution, and the observed signal may result from a few luminous sources lying just below the detection threshold. To investigate this, we plot the average distribution in counts for the sample of 147 stacked spectroscopic galaxies (Figure 1). Much of the high-end tail of the distribution results from random positive fluctuations. Only 3 sources consistently had > 7 counts. Removing those objects whose apertures have > 6 counts still results in a stacked signal with $S/N \sim 2.5$ and an average loss of 21 galaxies ($\sim 14\%$ of the sample). It is therefore likely that most of the stacked galaxies contribute to the signal, particularly given their wide range in optical, and likely X-ray, properties.

Contribution of low luminosity AGNs to the stacked signal is a concern. This is a problem with most X-ray stacking analyses, but we also possess the UV spectra for our sources. There are two objects undetected in X-rays for which the UV spectra show emission lines consistent with an AGN. Our ability to identify AGNs from their UV spectra regardless of their X-ray properties, and having identified only 2 such objects out of 149, suggests that subthreshold luminous AGNs do not contribute significantly to the stacked X-ray flux. Furthermore, UV selection biases against the dustiest sources so we do not expect to find many Compton-thick AGNs in our sample.

There are also two BM galaxies coincident with known

TABLE 1
RADIO AND X-RAY STACKING RESULTS

Sample	N_s[a]	$\langle z \rangle$[b]	S/N[c]	$F_{0.5-2.0\,\mathrm{keV}}$[d] ($\times 10^{-18}$ ergs cm^{-2} s^{-1})	$L_{2.0-10\,\mathrm{keV}}$[e] ($\times 10^{41}$ ergs s^{-1})	$S_{1.4\,\mathrm{GHz}}$[f] (μJy)	$L_{1.4\,\mathrm{GHz}}$[g] ($\times 10^{22}$ W Hz^{-1})	νL_ν[h] ($\times 10^{10}$ L$_\odot$)
BX+BM	147	2.09	8.9	5.65 ± 0.68	2.11 ± 0.25	2.30 ± 0.65	5.90 ± 1.66	3.50
BX	109	2.22	6.8	4.83 ± 0.79	2.09 ± 0.34	2.09 ± 0.75	6.17 ± 2.21	3.86
BM	38	1.71	6.0	8.04 ± 1.34	1.84 ± 0.31	...	...	2.46
$1.5 < z \leq 2.0$	54	1.82	5.6	6.89 ± 1.27	1.84 ± 0.33	...	...	2.81
$2.0 < z \leq 2.5$	73	2.24	6.0	5.24 ± 0.96	2.33 ± 0.43	...	...	4.05
$2.5 < z \leq 3.0$	43	2.87	3.3	4.21 ± 1.46	3.40 ± 1.18	...	...	4.61

[a]Number of galaxies stacked

[b]Mean redshift

[c]Signal-to-noise calculated in a manner analogous to that in Nandra et al. 2002

[d]Average soft-band X-ray flux per object

[e]Average rest-frame X-ray luminosity per object, assuming $\Gamma = 2.0$ and $N_\mathrm{H} = 1.6 \times 10^{20}$ cm^{-2}, for our adopted cosmology

[f]Average integrated radio flux density per object

[g]Average rest-frame 1.4 GHz luminosity per object, assuming synchrotron spectral index of $\gamma = -0.8$

[h]Average UV luminosity computed from G and $\mathcal{R}$ magnitudes approximating the 1600 and 1800 Å fluxes, respectively.

TABLE 2
STAR FORMATION RATE ESTIMATES

Sample	$\mathrm{SFR_X}$ (M$_\odot$ yr^{-1})	$\mathrm{SFR_R}$ (M$_\odot$ yr^{-1})	$\mathrm{SFR_{UV}^{cor}}$ (M$_\odot$ yr^{-1})	$\mathrm{SFR_X/SFR_{UV}^{uncor}}$
BX+BM	42	56	50	4.5
BX	42	58	54	4.2
BM	37	...	38	4.8
$1.5 < z \leq 2.0$	37	...	49	4.3
$2.0 < z \leq 2.5$	47	...	57	4.4
$2.5 < z \leq 3.0$	68	...	70	4.7
$\mathrm{SFR_{UV}^{cor}} \leq 20$ M$_\odot$ yr^{-1}	14	...	11	2.3
$20 < \mathrm{SFR_{UV}^{cor}} \leq 40$ M$_\odot$ yr^{-1}	40	...	38	4.4
$40 < \mathrm{SFR_{UV}^{cor}} \leq 60$ M$_\odot$ yr^{-1}	44	...	48	4.7
$\mathrm{SFR_{UV}^{cor}} > 60$ M$_\odot$ yr^{-1}	72	...	73	5.1

radio sources that are not detected in X-rays and are not included in the stacked samples. Removing such objects ensures excluding radio-loud AGN that might have unassuming UV and X-ray properties. For comparison, the 3 σ radio sensitivity is sufficient to detect SFR$\gtrsim 170$ M$_\odot$ yr^{-1}, a factor of 4 higher than the median SFR of our sample based on the X-ray or de-reddened UV SFR estimates. The stacked X-ray emission indicates a SFR of ~ 42 M$_\odot$ yr^{-1}. The on-axis soft-band flux limit implies a sensitivity to SFR$\gtrsim 186$ M$_\odot$ yr^{-1} at $z \sim 2$, a factor of 4.5 higher than the average SFR for spectroscopic $z \sim 2$ galaxies. Stacking the radio flux for the full spectroscopic sample indicates average SFRs from $33 - 70$ M$_\odot$ yr^{-1} depending on which estimator is used: the Bell (2003), Condon (1992), and Yun et al. (2001) calibrations give low, high, and median (~ 56 M$_\odot$ yr^{-1}) values, assuming $\gamma = -0.8$. We adopted the Yun et al. (2001) conversion (corrected for a binning error) as it is most relevant to the radio luminosity range considered here.

4.3. *Bolometric Properties of $z \sim 2$ Galaxies*

The UV-implied reddening indicates $A_V \sim 0.5$ mag and $N_H \sim 7.5 \times 10^{20}$ cm^{-2} assuming the Galactic calibration (Diplas & Savage 1994). For this column density, absorption in the $2 - 10$ keV band is negligible, and we therefore assume that SFR$_X$ is indicative of the bolometric SFR. In this case, we find a good agreement between the SFRs determined from the X-ray, radio, and de-reddened UV luminosities (L_X, $L_{1.4\ \rm GHz}$, and L_{UV}), suggesting that the locally-calibrated relations between specific luminosity and SFR remain valid within the uncertainties at $z \sim 2$, under the caution that we cannot independently test for these relations as we have no direct measure of L_{bol}.

The $\langle L_X \rangle$ and $\langle L_{1.4\ \rm GHz} \rangle$ of spectroscopically identified $z \sim 2$ galaxies are comparable to those of local starbursts. The X-ray/FIR relation for local galaxies (Ranalli et al. 2003) implies $\langle L_{FIR} \rangle \sim 2.6 \times 10^{11}$ L$_\odot$. The stacked $L_{1.4\ \rm GHz}$ implies $\langle L_{FIR} \rangle = 1.1 \times 10^{11}$ L$_\odot$ (Yun et al. 2003). These estimates are similar to the FIR luminosity of luminous infrared galaxies (LIRGs), and are expected to have $S_{850\mu m} \sim 0.3$ mJy (e.g., Webb et al. 2003) and would therefore be missing in confusion-limited SCUBA surveys to 2 mJy. SIRTF will have the same rest-frame 7 μm sensitivity to $z \sim 2$ galaxies as ISO has at $z \sim 1$ for $L_{FIR} \gtrsim 5 \times 10^{10}$ L$_\odot$ galaxies (e.g., Weedman, Charmandaris, & Zezas 2004; Flores et al. 1999). Therefore, unlike the stacked averages presented here, the SIRTF data will be the first extinction-free tracer of the SFR distribution of the $z \sim 2$ sample as the stacked galaxies should be individually detected at 24 μm.

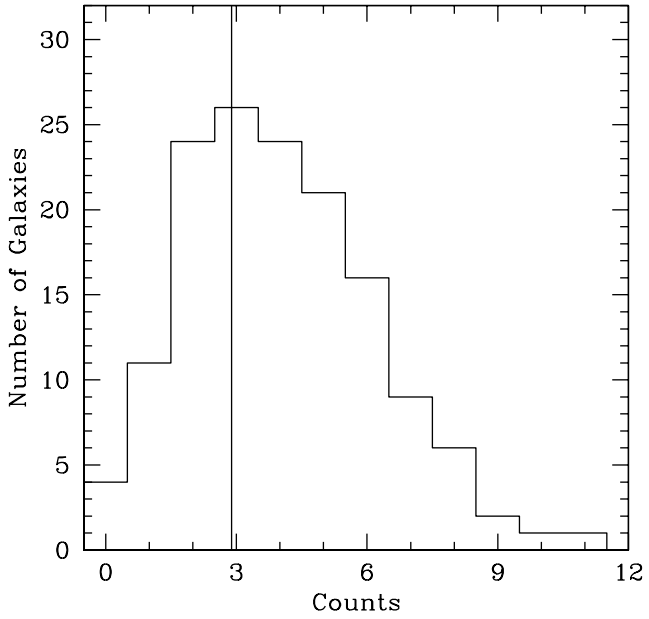


FIG. 1.— Average distribution of counts for the spectroscopic sample. The vertical line denotes the average background count per aperture. The number excess at high counts (> 7) results from random positive fluctuations.

For a fair comparison between the three redshift bins for $1.5 < z \lesssim 3.0$, we have added back those direct X-ray detections in the stacks for the $1.5 < z \leq 2.0$ and $2.0 < z \leq 2.5$ samples that would not have been detected if they had $z > 2.5$. There were no such sources with $1.5 < z \leq 2.0$ and only one with $2.0 < z \leq 2.5$, increasing $\langle L_{2-10\ \rm keV} \rangle$ by 2% to 2.38×10^{41} ergs s^{-1}.

The distance independent ratio SFR$_X$/SFR$_{UV}^{uncor}$ (Table 2) is similar among the selection and redshift subsamples indicating that on average *UV-estimated SFRs (uncorrected for extinction) are a factor of* ~ 4.5 *times lower than the bolometric SFRs for galaxies between redshifts* $1.5 < z \leq 3.0$. For comparison, Nandra et al. (2002) find this factor to be ~ 5 for both the $z \sim 1$ BBG and $z \sim 3$ LBG populations, and the factor is comparable to that of local starburst galaxies (Seibert et al. 2002). The attenuation computed for the BX/BM sample using the Calzetti et al. (2000) extinction law is similar to that computed from SFR$_X$/SFR$_{UV}^{uncor}$. The de-reddened UV-estimated SFRs (SFR$_{UV}^{cor}$) agree well with those predicted from the radio continuum for the two samples for which radio estimates could be obtained. Finally, we note the factor of ~ 5 UV attenuation is similar to that advocated by Steidel et al. (1999) for UV-selected samples at all redshifts.

The average attenuation factor increases as the SFR increases, as shown by the last 4 subsamples in Table 2, and is expected if galaxies with higher SFRs have greater dust content on average (e.g., Adelberger & Steidel 2000). SFR$_{UV}^{cor}$ follows the bolometric SFR even for low luminosity systems, indicating that the observed correlations are not entirely driven by only the most luminous galaxies.

5. CONCLUSIONS

We have made significant progress in estimating and comparing SFRs determined from UV, X-ray, and radio emission from galaxies between redshifts $1.5 \lesssim z \lesssim 3.0$, postulated to be the most "active" epoch for galaxy evolution. The locally-calibrated SFR relations, though uncertain in individual systems, appear to remain statistically valid at high redshift. Stacking the X-ray and radio emission from UV-selected galaxies at $z \sim 2$ indicates that these galaxies have an average SFR of ~ 50 M$_\odot$ yr^{-1} and an average UV attenuation factor of ~ 4.5. The prospect of increased radio sensitivity with the E-VLA, as well as X-ray campaigns in different fields to similar depth as the 2 Msec survey in the GOODS-North field, will allow for a more direct probe of the radio and X-ray flux distribu-

tion for the stacked galaxies. SIRTF/MIPS 24 μm data for the GOODS-N field will trace the dusty star formation in $z \sim 2$ galaxies and allow for the cross-checking of the results presented here.

We thank Alice Shapley, Dawn Erb, Matt Hunt, and Kurt Adelberger for help in obtaining the data presented here. CCS has been supported by grants AST 0070773 and 0307263 from the National Science Foundation (NSF) and by the David and Lucile Packard Foundation. NAR acknowledges support from a NSF Graduate Research Fellowship.

REFERENCES

Adelberger, K. L., & Steidel, C. C. 2000, ApJ, 544, 218
Adelberger, K. L., Steidel, C. C., Shapley, A. E., Hunt, M. P., Erb, D. K., Reddy, N. A., & Pettini, M. 2004, submitted to ApJ
Alexander, D. M., Bauer, F. E., Brandt, W. N., Schneider, D. P., Hornschemeier, A. E., Vignali, C., Barger, A. J., Broos, P. S., et al. 2003, AJ, 126, 539
Bell, E. F. 2003, ApJ, 586: 794
Brandt, W. N., Hornschemeier, A. E., Schneider, D. P., Alexander, D. M., Bauer, F. E., Garmire, G. P., & Vignali, C. 2001, ApJ, 558, 5
Calzetti, D., Armus, L., Bohlin, R. C., Kinney, A. L., Koornneef, J., & Storchi-Bergmann, T. 2000, ApJ, 533, 682
Chapman, S. C., Blain, A. W., Ivison, R. J., & Smail, I. R. 2003, Nature, 422, 695
Condon, J. J. 1992, ARA&A, 30, 575
Di Matteo, T., Croft, R. A. C., Springel, V., Hernquist, L. 2003, ApJ, 593, 56
Diplas, A. & Savage, B. D. 1994, ApJS, 93, 211
Feigelson, E. D., Broos, P. S., Gaffney, J. A. III, Garmire, G., Hillenbrand, L. A., Pravdo, S. H., Townsley, L., & Tsuboi, Y. 2002, ApJ, 574, 258
Flores, H., Hammer, F., Thuan, T. X., Césarsky, C., Desert, F. X., Omont, A., Lilly, S. J., Eales, S., et al. 1999, ApJ, 517, 148
Gallego, J., Zamorano, J., Arag'on-Salamanea, A., & Rego, M. 1995, ApJ, 455, 1
Giavalisco, M., Ferguson, H. C., Koekemoer, A. M., Dickinson, M., Alexander, D. M., Bauer, F. E., Bergeron, J., Biagetti, C., et al. 2004, ApJL, 600, 93
Kennicutt, R. C. 1998a, ARA&A, 36, 189
Kennicutt, R. C. 1998b, ApJ, 498, 541
Kim, D.-W., Fabbiano, G., & Trinchieri, G. 1992, ApJ, 393, 134
Meurer, G. R., Heckman, T. M., & Calzetti, D. 1999, ApJ, 521, 64
Nandra, K., Mushotzky, R. F., Arnaud, K., Steidel, C. C., Adelberger, K. L., Gardner, J. P., Teplitz, H. I., & Windhorst, R. A. 2002, ApJ, 576, 625
Oke, J. B., Cohen, J. G., Carr, M., Cromer, J., Dingizian, A., Harris, F. H., Labrecque, S., Lucinio, R., et al. 1995, PASP, 107, 375
Ranalli, P., Comastri, A., & Setti, G. 2003, A&A, 399, 39
Richards, E. A. 2000, ApJ, 533, 611
Seibert, M., Heckman, T. M., Meurer, G. R. 2002, AJ, 124, 46
Stark, A. A., Gammie, C. F., Wilson, R. W., Bally, J., Linke, R. A., Heiles, C., & Hurwitz, M. 1992, ApJS, 79, 77
Steidel, C. C., Adelberger, K. L., Giavalisco, M., Dickinson, M., & Pettini, M. 1999, ApJ, 519, 1
Steidel, C. C., Shapley, A. E., Pettini, M., Adelberger, K. L., Erb, D. K., Reddy, N. A., & Hunt, M. P. 2004, submitted to ApJ
Webb, T. M., Eales, S., Foucaud, S., Lilly, S. J., McCracken, H., Adelberger, K., Steidel, C., Shapley, A., et. al. 2003, ApJ, 582, 6
Weedman, D., Charmandaris, V., & Zezas, A. 2004, ApJ, 600, 106
Yun, M. S., Reddy, N. A., & Condon, J. J. 2001, ApJ, 554, 803